Computational Neuroscience of Synapses and Neurons

116

Adam J. H. Newton, Samuel A. Neymotin, Cliff C. Kerr, and William W. Lytton

Contents

A. J. H. Newton
Department of Physiology and Pharmacology, State University of New York Downstate Health Sciences University, Brooklyn, NY, USA

Department of Biostatistics, Yale University, New Haven, CT, USA

Yale Center for Medical Informatics, Yale School of Public Health, New Haven, CT, USA
e-mail: adam.newton@downstate.edu

S. A. Neymotin
Center for Biomedical Imaging and Neuromodulation, Nathan S. Kline Institute for Psychiatric Research, Orangeburg, NY, USA

Department of Psychiatry, New York University Grossman School of Medicine, New York, NY, USA
e-mail: samuel.neymotin@nki.rfmh.org

C. C. Kerr
Complex Systems Group, School of Physics, University of Sydney, Sydney, Australia

Institute for Disease Modeling, Global Health Division, Bill & Melinda Gates Foundation, Seattle, WA, USA
e-mail: cliffk@neurosim.downstate.edu

W. W. Lytton (✉)
Physiology and Pharmacology, State University of New York Downstate Medical Center, Brooklyn, NY, USA
e-mail: billl@neurosim.downstate.edu

D. W. Pfaff et al. (eds.), *Neuroscience in the 21st Century*,
https://doi.org/10.1007/978-3-030-88832-9_86

Abstract

A fundamental unit in biology is the cell, and the fundamental information processing unit in neuroscience is believed to be the neuron. Computer simulation of neurons depends on a series of transformations that provide different ways of looking at the same set of phenomena, from the biophysical concepts of ion flow, second messenger diffusion/reaction cascades, to the electrical concepts of resistance and capacitance, to differential equations and their numerical simulation, to information theory and systems engineering. Electronically, the neural membrane acts as a capacitor, while protein pores act as resistors. To this basic picture, many types of complexity can be added. Real neurons are not simply a single capacitor and resistor but rather many capacitors, resistors, and batteries, leading to the parallel conductance model and to multicompartment models. Using these models, given current concentrations of ions inside and outside the cell, one can calculate the voltage for a given neuron at a given point in time. However, voltages change with time and are the tip of a much more complex dynamical system. The voltage at any given time depends on the state of voltage and ligand-sensitive ion channels on the membrane, i.e., which pores are open and which are closed. Simulations can demonstrate how the neuron's state evolves over time as a dynamical system. In this chapter, the genesis of the action potential and the spread of signals through the cell are explored.

Keywords

Cell membrane · Compartmental model · Computational neuroscience · Compartmental modeling · History · Current clamp · Kirchhoff's law · Lipid membrane · Parallel conductance model · Resting membrane potential (RMP) · State variable

Brief History

Computational neuroscience is made up of a variety of strands, sometimes competing with one another for dominance. The strands have arisen due to the confluence of a set of different founding fields with different approaches and assumptions – engineering, math, physics, biology, computer science, psychology, and others. Another factor that has contributed to the failure of the strands to congeal into a single field is the lack of major recent success in any one of them. A crucial breakthrough in our understanding of the brain would set up a clear research direction ("a dominant paradigm" in Kuhn's phrase) that other researchers would readily follow.

The following strands can be identified: (1) Computational neuroscience arising from computer science. This strand focuses on the computational capacities of brain-like networks. This strand has given rise to the field of artificial neural networks (ANNs) (Churchland and Sejnowski 1994), deep neural networks (DNNs) an ANN with multiple hidden layers, and convolutional neural networks (CNNs) a form of DNNs which include layers where a convolution filter rather than summation is applied to the inputs, inspired by receptive fields in the visual cortex. (2) Theoretical neuroscience arising from physics. This strand attempts to understand neural systems in the context of closed-form solutions: simple but potent sets of equations that describe the basics of a system. Ideas in this strand tend to parallel those in other branches of physics, such as statistical mechanics, chaos theory, and wave theory. In these studies, computer models are typically used as a tool but are not an end in and of themselves. A major success in this strand has been the development of the notion of attractors in the nervous system, an idea that can be traced back to Hopfield. (3) Systems biology arising from the many omes: genome, proteome, interactome, etc. These studies yield vast quantities of information that cannot be manually organized but must be pulled together in databases (bioinformatics). From there, they can only be understood as a system by using computational models that revivify the data by putting them in a relative context. Neuroinformatics and multiscale brain modeling are active approaches that have arisen from this strand. (4) Biophysical computation arising from the grand traditions of a line of famous Nobel Prize winners: Hartline, Ratliffe, Hodgkin, Huxley, and others. The basis of this approach is in the functioning of the single nerve cell with an emphasis on its electrical characteristics. Part of the reason for this electrical bias is that the founders of this strand were electrophysiologists who built their own amplifiers and were therefore very conversant with electrical representations.

Overall, the four strands can be characterized as to whether they are top-down or bottom-up. The top-down approach arises from an engineering perspective: design a machine to perform a particular task. If you are interested in intelligence, then design an artificial intelligence machine. The top-down approach is mostly utilized in strands 1 and 2. The bottom-up perspective is the province of the phenomenologist or the taxonomist: collect data and organize it. This is the approach in strands 3 and 4. This chapter, on neuron modeling, primarily takes the perspective of strand 4. The next chapter, on neuronal network modeling, widens out to include strand 3. The perspectives of strand 1 and 2 are underrepresented here. A good introduction to strand 1 is the first section of the textbook by Lytton (2002) or the more detailed treatment by Hertz (2018) or Trappenberg (2010). A good introduction to strand 2 is Dayan and Abbot (2001).

While the choice of focus here may seem to be an endorsement of bottom-up thinking, it should not be taken this way. Overall, the authors regard a *middle-out*, and multiscale, approach as best, incorporating top-down thinking while creatively utilizing bottom-up data. This perspective will become more apparent in the next chapter. We have taken the bottom-up approach in this chapter for didactic reasons: it is prudent to start with the basics. These basics will take us from chemistry and biochemistry, through electrical engineering, into numerical calculus and emerge finally into an account of the electrical activity of a neuron.

One key advantage of a computational study is its accessibility. Unlike other areas of science, the computational study does not require specialized equipment. All of the simulations shown in this chapter can be readily performed on a small laptop. Several of these are available as the simulations that accompany the textbook *From Computer to Brain*. This chapter focuses on computational techniques. This will allow the reader to really understand the thinking underlying the science rather than simply seeing the results.

Modeling Membranes: The Conceptual Model

The cell exists because it has managed to separate its inside from the outside. Within a neuron, as in other eukaryotic cells, the cell is a bag of jelly within which are other bags of jelly: nucleus, mitochondria, endoplasmic reticulum, etc. Just like gelatin that you eat, this jelly is made up of proteins and water. The key to the electrical properties of biological tissue is that this water is salt water and the ions of these salts conduct electricity. These ions, electrically charged particles, are either positive (Na^+, K^+, Ca^{2+}, and others) or negative (Cl^- and $HCO_3{}^-$). Charge makes the ion hydrophilic since the hydrogen of H_2O will form hydrogen bonds with the negative charge, while the oxygen will stay near a positive charge. Fat will only accommodate uncharged molecules. Therefore, the ions and other charged proteins can move around freely in either extracellular or intracellular space. With salt water both inside and outside, electricity flows freely through these media. The membrane, however, is fat, also called lipid. Ions will not pass through fat unaided, just as oil (fatty) and water (dipolar, hence piecewise charged) do not mix. In fact, the fancy word for fatty is *hydrophobic*: water-fearing. Correspondingly, the salt water is a hydrophilic (water-loving) zone. Conversely, one can speak of substances as being lipophilic or lipophobic relative to lipid. Some proteins are hydrophobic and can float around within the membrane itself. They are trapped there and will not move into the water on either side. Other proteins are purely hydrophilic and float around in the cytoplasm inside the cell. Other proteins have both hydrophilic and hydrophobic parts and thus join or span the membrane.

Figure 1 shows the standard model of the cell membrane. The fatty part of each phospholipid molecule points into the interior of the membrane (labeled as intramembranous), away from the water that is both inside and outside. Lipophilic substances can float around inside the membrane. The cross-hatched green-orange object in the figure is lipophilic (hydrophobic), either a protein or an intramembrane chemical messenger. In general, proteins are the active machinery of cells, involved in metabolism, cell reproduction, and practically every other function.

Specialized proteins act as extracellular receptors for neurotransmitters. A receptor is sensitive to a specific neurotransmitter. In general, receptors can be classified as ionotropic or metabotropic. Ionotropic receptors are membrane-spanning protein pores, as shown in Fig. 1. Such a protein will align itself according to its hydrophilic and hydrophobic parts. In so doing, the protein can provide a tunnel that allows ions to pass through from inside to outside or vice versa. Note that ions cannot move directly across the membrane but only flow through these protein pores.

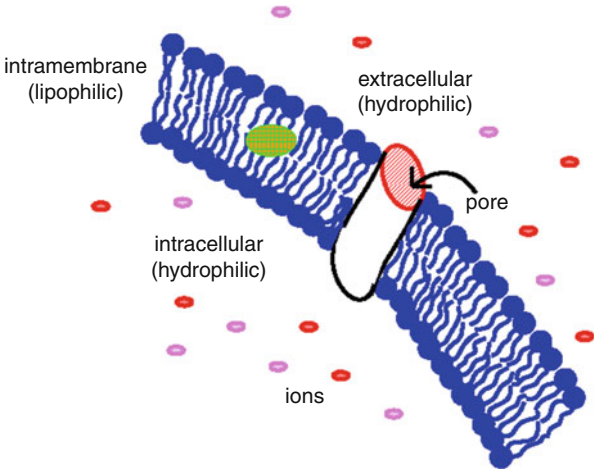

Fig. 1 The cell membrane (*blue*) has an intramembranous lipid interior made of phospholipid tails. On either side of the membrane, the environment is hydrophilic (watery) and can accommodate positive (*red*) and negative (*purple*) ions that carry current. This is also where hydrophilic proteins are found. Lipophilic proteins (*green-orange ellipse*) and other lipophilic substances can float around inside the membrane. Membrane-spanning proteins have both lipophilic and hydrophilic parts and orient themselves across the membrane (*white*). They can form pores or tunnels (*red*) that allow ions to move in or out of the cell

Metabotropic receptors also connect to spanning proteins, but instead of acting as pores, they release chemicals intracellularly celled *second messengers.* Second messengers include cAMP, G proteins and others. Second messengers often connect with third, fourth, etc. messengers, forming complex signaling cascades. These messengers may go on to open ion channels, combine with other signaling cascades or activate enzymes. The membrane-spanning proteins are very sophisticated machines. They can open and close according to different signals, thereby allowing ions to either enter or not.

Modeling Transformation #1: From Membrane to Electrical

As noted above, there are many types and styles of modeling. One important aspect of the problem that determines the modeling approach is the scale of the model required. At the nanoscale, separate models have been developed to describe the extracellular space, to describe the intramembranous lipid environment, and to describe individual pores and even parts of pores. This chapter explores computer modeling at this scale. However, notice that Fig. 1 is itself a model, a conceptual model portrayed graphically and verbally. This conceptual model is a necessary first step in translating a physical system into a computational model. In this instance, the conceptual model provides connections between the concepts (and models, if they exist) of pores, membranes, cytoplasm, and extracellular space. Notice that descriptions like this are both model and metaphor: extracellular space is jelly, proteins form

tunnels. You will notice that these models/metaphors necessarily always lack detail and are always to some degree, inaccurate. This is a general property of models that is often not appreciated: they are limited. They are never quite right. However, they can be useful when they are "right enough."

We now make the transition from one limited model to another limited model. The model in Fig. 1 becomes the model in Fig. 2. The extracellular fluid becomes ground, a place where current can always be either placed or taken from (a sink or source for current). The pore becomes a resistor (also called a conductor) – it allows current to pass but somewhat limits its passage. In some cases, this resistor will be a variable resistor ("rheostat"), with the possibility of controlling the amount of current that is allowed to pass through. The cytoplasm is highly conductive, so it can be represented just as a wire connector. The lipid membrane itself serves as an insulator tucked in between two electrically conducting plates. This is the design of a capacitor. In electronics, a capacitor is built by placing an insulating material between two parallel metal plates that are attached to the wire leads of the capacitor. Since these plates do not touch, electricity (charge) does not pass directly through the capacitor but flows indirectly as one plate induces electrical flow in the other plate. The two parallel lines in the standard symbol for the capacitor (Fig. 2) represent these two plates. A capacitor has special properties which are of interest in our understanding of the nervous system, a first stage of providing a connection between mechanism and function. Capacitance provides a low-level, short-lived form of memory.

Ions moving through water carry charge. Movement of charge is called current. Benjamin Franklin's definition, still used, defines positive current as of the movement of positive charge. This seems counterintuitive in metal wires, where the charge carriers are the negative electrons. However, some of the biological carriers

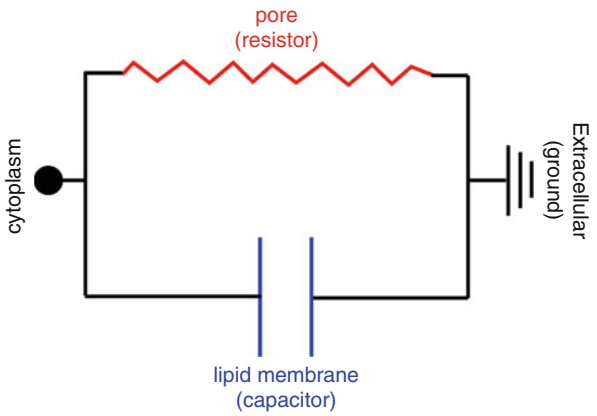

Fig. 2 Morph of Fig. 1 into an equivalent circuit. The lipid membrane becomes a capacitor (*blue*). The pore becomes a resistor (*red*). Some pores will be controllable and will be shown as rheostats (variable resistors). The outside becomes a connection to *ground*. The cytoplasm becomes a simple wire – here represented with a little *circle* at the end for a connector. The whole thing represents what is called an RC (resistor-capacitor) circuit in electronics

are positive ions: Na^+, K^+, and Ca^{2+}. Current flows through wires freely and through resistors with some resistance (hence the name). Charge is neither created nor destroyed (Kirchhoff's first law), but ground provides a place from which current can always be obtained or placed. Kirchhoff's law will be particularly important for making the modeling transformation #2, from the circuit diagram to algebra. Kirchhoff's law tells us that current placed anywhere in the circuit has to go somewhere, i.e., conservation of current. Like the laws of conservation of mass and energy in their respective domains, this law says that all stuff comes from somewhere and goes somewhere. Kirchhoff's law says that current recycling is required as long as you stay within the circuit. Note that current does not disappear when going to the ground, it just dissipates. Ground is an inexhaustible landfill: in any circuit which is grounded, current will eventually go to ground.

Figure 3 shows how Kirchhoff's law is applied. Current (I) is measured in amperes (amps or A), which represents the flow of charge (Q) over time. If a circuit divides into two wires, as here, the current will divide equally where the two wires separate. Half of the 3 amps go down one branch, and other half go down the other. When the wires come back together, the currents add back up. Charge is conserved; current is conserved. From the positive voltage (or potential) at the bottom of Fig. 3, positive current flows "downhill" to the ground. Ground always remains at 0 V (by definition). Conversely, if the side of the circuit away from the ground were held at a negative voltage, the current would flow out of ground down to this more negative potential. In a more complicated case, such as Fig. 2, the current will divide unequally. When the current divides like this, it is following parallel paths. In general, electrical components – wires, resistors, capacitors – are arranged either in parallel or in series. In Fig. 2, the resistor and capacitor are in parallel, i.e., they are on parallel wires in the circuit. Components in series would be arranged one after the other.

After Kirchhoff's law, there are two other laws of importance: one for resistance and the other for capacitance. Ohm's law of resistance is the best known: $V = IR$, i.e., voltage equals current times resistance. For neurobiological modeling, conductance g, the inverse of resistance *R, is used*. Mathematically, conductance is defined as $g = \frac{1}{R}$. Since resistors allow some current to flow, they can be described either in terms of how much current they let through (conductance) or how much they stop (resistance). Resistance is expressed in ohms (Ω) and is represented by R.

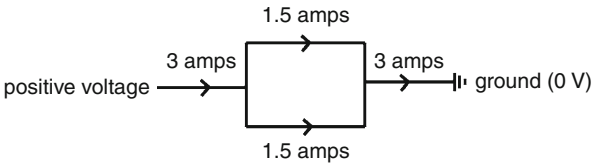

Fig. 3 Kirchhoff's current law. Since charge can be neither created nor destroyed, all current that goes into a circuit must go somewhere. If 3 amp are added to the *left side* of the circuit, there must also be 3 amp in the middle of the circuit (in this example, two parallel wires each carrying 1.5 amp) and 3 amp leaving to ground

Conductance is measured in siemens (*S* or mho, which is ohm spelled backward) and is represented by *g*. Whatever you call it, the same sawtooth resistor symbol is used. Ohm's law can be expressed in terms of conductance as $V = I/g$; hence, $I = gV$. Ohm's law establishes a *linear relationship* between current and voltage. The larger the voltage difference between the two sides of the resistor, the more current will flow. In the circuit diagram of Fig. 2, the pores of a single type are all lumped together as a single big conductor. This is another example of the simplification characteristic of multiscale modeling: millions of tiny pores are represented here as one conductor (red in Fig. 2). This ubiquitous conductance is known as the leak conductance, g_{leak}, and is caused by ions leaking into or out of the cell via transmembrane pores.

Capacitance means the *capacity* to hold charge. The governing equation for a capacitor is $Q = CV$, i.e., charge equals capacitance times voltage. The relation of current to voltage across a capacitor involves movement or change in time since current *I* is the flow of charge *Q*. The law of capacitance states that current flow is proportional to the rate of change of voltage. A capacitor will pass current easily in the presence of a quickly changing voltage but will not pass any current in the presence of constant voltage. In electronics, capacitors are commonly used to store energy or information. The cell membrane has both these functions.

A resistor (R) and capacitor (C) arranged in parallel are called an RC circuit (Fig. 2). The RC circuit is a fundamental element of study in electronics as well as in electrophysiology. In electronics, one would test an RC circuit by providing a signal on the side of the circuit away from ground. Either one injects current and measures voltage, or one provides a known voltage and looks at the flow of current. In electrophysiology, one can do the same thing. We typically insert a glass electrode through the membrane to reach the side of the circuit away from the ground. We then inject current into the inside of the cell and measure the voltage across the membrane. This is called *current clamp* (the word clamp here means that one maintains a constant current). Alternatively, one can measure the amount of current one must add ("source") or remove ("sink") through the electrode in order to maintain a constant voltage: *voltage clamp*. In either case, charge added to the inside of the cell passes out through the protein pores (conversely, charge removed from the cell flows back in through the pores). Once the current reaches the outside of the cell, it will disperse to the rest of the body and the surrounding world to ground.

Modeling Transformation #2: From Electrical to Equations

We now have the three laws needed (Kirchhoff's law, Ohm's law, rule of capacitance) to create a set of algebraic and differential equations. Differential equations are generally understood using calculus. However, we are heading toward a numerical solution of the differential equations, a solution that directly uses numbers, in the next transformation. Such numerical solutions are handled on computers. Computers cannot directly handle the infinitesimals of calculus because infinitesimals are not

numbers at all but are mathematical representations of the infinitely small. Although calculus remains the most important tool for understanding differential equations, it is not needed for our current description or for computer simulation. Just as a cashier uses a computer (the modern cash register) to sell 15 light bulbs without necessarily remembering how to multiply by 15, so can the computer user solve sophisticated differential equations without remembering the theory of differential equations.

The capacitance law given above is $Q = CV$. Current, I, is the change in charge, Q, with time. The capital Greek letter delta (Δ) is use to mean change. A change in time (t) between two times, now and before, is represented as the difference in time $\Delta t = t_{\text{now}} - t_{\text{before}}$. For a shorthand, we will call the earlier of the two times ("before") time a, and the later one ("now") time b, so $\Delta t = t_b - t_a$. Similarly, the change in charge during that same period is $\Delta Q = Q_b - Q_a$. The difference between this algebraic treatment and the classical calculus treatment is that the values used here are numbers representing actual quantities or durations. So if t_a is 4:44:32 PM and t_b is 4:44:35 PM, then Δt is 3 s. Since the current is the amount of change in charge over time, we can represent it as $I = \frac{\Delta Q}{\Delta t}$. ΔQ divided by Δt is the rate of change of the charge – how quickly the charge is changing or how much it is flowing. This is directly analogous to the calculation of velocity as the amount of change in location (Δx) divided by Δt.

Now one can transform the capacitance equation for charge into a capacitance equation for current: $Q = CV$. At time t_a, $Q_a = CV_a$ and at time t_b, $Q_b = CV_b$. We subtract the left and right sides of the equations: $Q_b - Q_a = C(V_b - V_a)$, so $\Delta Q = C\Delta V$. We then divide both sides by the time that has passed: $\frac{\Delta Q}{\Delta t} = C\frac{\Delta V}{\Delta t}$. Since $I = \frac{\Delta Q}{\Delta t}$, the law of capacitance can be expressed in terms of current as $I = C\frac{\Delta V}{\Delta t}$.

This is the final equation needed to generate the full set of model equations which transforms the electronics model of Fig. 2 into algebra. As in Fig. 3, we will inject a current I_{in} at the bottom of the circuit in Fig. 2. We will then see what happens to that current. It will either go through the capacitor or through the resistor to get to ground. (Remember that although *current* can pass through a capacitor, *charge* cannot – it accumulates on one side of the capacitor, which pushes charges away from the opposite side, thereby creating a current.) Arithmetically, $I_{\text{in}} = I_{\text{C}} + I_{\text{R}}$, which are the currents through the capacitor and the resistor, respectively. I_{C} and I_{R} can be filled in using the corresponding equations:

$$I_{\text{in}} = C\frac{\Delta V}{\Delta t} + gV$$

The above is actually a discrete form of a basic ordinary differential equation that could be easily solved using calculus. However, we will solve it here using the computer through numerical integration. The reason for using numerical integration is not simply to avoid calculus. We need numerical integration because this is only a tiny piece of the full neuron model. The full system that we are interested in includes many more components. Once we build up to the whole neuron model, the analytic techniques of classical calculus would no longer be sufficient: numerical integration is necessary.

Modeling Transformation #3: From Equation to Simulation

A common question we will want to answer is: what is the voltage at the current time? To find out, first recall that $\Delta V = V_b - V_a$. Substituting this into the previous equation leaves us with

$$I_{\text{in}} = C\frac{V_b - V_a}{\Delta t} + gV_a$$

After a little rearrangement, we get an explicit expression for V_b, the voltage at the current time:

$$V_b = \left(1 - \frac{g\Delta t}{C}\right)V_a + \frac{I_{\text{in}}\Delta t}{C}$$

This is now in the form of an *update equation* that we could use in a computer program. We calculate voltage (V_b) based on current voltage V_a. At the same time, we can update time by simply adding Δt: $t_b = t_a + \Delta t$. These are both calculations that one can do on a calculator. We would then record the new time and voltage and would then update V_a and t_a to the new values in order to start again: the new voltage becomes the next V_a and the new time the next t_a, and we are ready for another update step. Note that although t_a and t_b do not explicitly appear in the equations above, we need to keep track of them in order to be able to interpret V_a and V_b – e.g., if we store all of the voltages and times as they are calculated, we can use them to make a graph of voltage versus time.

In standard neuron simulation, we use units of millivolts (mV) for voltage and milliseconds (ms) for time. In this example, let us set $g = 1$ mS/cm^2 and $C = 1$ μF/cm^2 for simplicity. (The common use of square centimeter for these units, contrasted with the common use of microns for neuron size, is an example of why unit analysis is important and such a nuisance.) Using these values, $\frac{g}{C} = 1/\text{ms}$. Similarly, for simplicity, we set the injected current to 1 μA/cm^2. We will use $\Delta t = 0.01$ ms. With these convenient choices, the update equation is

$$V_b = (1 - 0.01)V_a + 0.01$$

At every step, V_b will be updated according to this rule, and t_b will be increased by Δt. So the update for the full simulation requires equations for updating both t and V:

$$t = t + 0.01$$
$$V = 0.99 \cdot V + 0.01$$

Notice that we have now left out the a, b subscripts for V and t. This is common practice since this is the form the update rules will take when entered into a computer program.

We now just need a starting point, called the initial conditions, and we can simulate. We will start with $V = 0$ at $t = 0$. Then at $t = 0.01$, $V = 0.01$ and at $t = 0.02$, $V = 0.020$; $0.0099 + 0.01 = 0.0199$. Values during the first 100 μs are

t (ms)	V (mV)
0.00	0.000
0.01	0.010
0.02	0.020
0.03	0.030
0.04	0.039
0.05	0.049
0.06	0.059
0.07	0.068
0.08	0.077
0.09	0.086
0.10	0.096

This is known as the charging curve. Notice that the initial rise is very close to being linear. Figure 4 shows 5 ms of simulation and demonstrates the gradual deviation from linearity. In real life, the resting membrane potential (RMP) of a neuron would be about −65 mV, so we would start Fig. 4 at −65 mV instead of 0. The charging curve will look the same, just starting at −65 mV. The maximum value ($V_{\max}$) for the curve will be determined by resistance; higher resistance will give a higher final value. We can find this value by solving the update rule as a regular equation to get the steady state:

$$V_{\max} = 0.99V_{\max} + 0.01 \quad (1 - 0.99)V_{\max} = 0.01 \quad V_{\max} = 1 \text{ mV}$$

We can similarly solve for $V_{\max}$ in the parameterized equation to show that in general, $V_{\max} = \frac{I_{\text{in}}}{g}$. Notice that $V_{\max} = \frac{I_{\text{in}}}{g} = I_{\text{in}} \cdot R$. This is just Ohm's law. The value of this maximum reflects the fact that at the end, the voltage is not increasing.

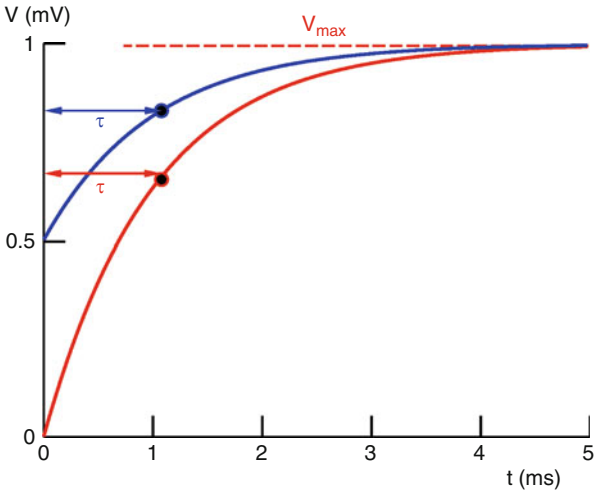

Fig. 4 Simulation of the RC circuit shown in Fig. 2, representing a membrane charging curve. Simulation parameters were $C = 1$ μF/cm^2, $g = 1$ mS/cm^2, $I_{\text{in}} = 1$ μA/cm^2. These give a time constant of $T_{\text{memb}} = [C/g] = 1$ ms and a maximum voltage of $V_{\max} = [(I_{\text{in}})/g] = 1$ mV. The two trajectories show different initial conditions: $V_0 = 0$ (*red*) or $V_0 = 0.5$ (*blue*)

Therefore, $\frac{\Delta V}{\Delta t} = 0$ and there is no capacitative current. All the current flows through the resistor, and the voltage is determined entirely by Ohm's law. Another important aspect of the charging curve is how quickly the charging takes place. This rate of climb is measured as T_{memb}, the time constant. Using calculus, the time constant can be shown to be equal to resistance times capacitance: $T_{\text{memb}} = \text{RC} = \frac{g}{C}$. In Fig. 4, $T_{\text{memb}} = 1$ ms. This is the time required for the voltage to reach roughly 63% (i.e., $1/e$) of the maximum voltage V_{max}.

We cannot directly measure capacitance and membrane conductance in real neurons. However, both V_{max} and T_{memb} can be measured by injecting current into a cell from an electrode. One then measures the voltage difference between the inside and outside of the cell to estimate g_{memb} and C_{memb}. Inverting the above equations, we see that $g_{\text{memb}} = \frac{I_{\text{in}}}{V_{\text{max}}}$ (Ohm's law) and $C_{\text{memb}} = I_{\text{in}}/(V_{\text{max}} \cdot T_{\text{memb}})$. Hence, although g_{memb} and C_{memb} are the basic parameters used in the simulations, these are only estimates based on measured cell properties.

Figure 4 represents the simulation of a simple *dynamical system*. The word dynamics and the term dynamical system, originally applied to systems in motion such as the planets, have been generalized to refer to any system in which quantities change with time. In this case, voltage, V, changes with time. In studying dynamical systems, we distinguish between state variables and parameters. State variables describe the state of a dynamic system and are typically defined by differential equations. Here, voltage is the only state variable. Parameters are usually fixed values that influence how the states change over time: the parameters here are g, C, and I_{in}. The other key attributes for a dynamical system are initial conditions. In this case, if we set voltage to a different starting point, we will get a different result. Two trajectories are shown in Fig. 4. The red curve shows a trajectory with an initial condition of $V = 0$, while the blue curve shows trajectory with an initial condition of $V = 0.5$. Notice that the key dynamical characteristics, V_{max} and T, remain the same regardless of initial conditions.

Modeling Transformation #4: From Simulation to Information Processing

We are interested in how the physical properties of a neuron provide its information processing capabilities. In Fig. 4, a continuously injected current provides an input signal. It is customary to consider this situation in the context of *signals and systems*, a subfield of engineering. The system, in this case, the membrane model, transforms the signal by filtering it. In this case, the response of the membrane depends on the two fundamental properties of capacitance and resistance. There are many biological actions that can alter membrane resistance. Stepping back a couple of transformations to the underlying conceptual model, we will recall that membrane resistance is dependent on the pore shown in Fig. 1. These pores can be open or closed by a variety of influences: neuromodulators, synaptic inputs, voltage changes, phosphorylation from kinases, ongoing activity, second messengers, etc. By contrast, there is

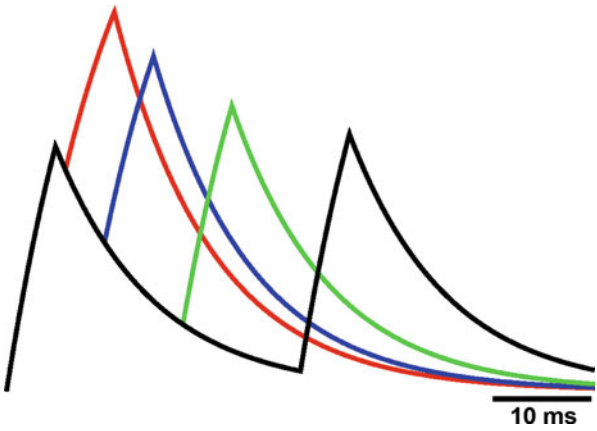

Fig. 5 A second signal is delivered to the membrane at various times (1, 5, 13, and 25 ms) following an initial signal. Each signal is of the same amplitude. The more quickly the second signal arrives following the first, the larger the resultant voltage

no known mechanism that would change membrane capacitance on the time scale relevant to neural signaling.

Having set the parameters of our system and seen the response to a single signal, we can now look at the response to multiple signals. The fundamental property that the membrane shows is literally the *capacity* for signal summation: the capacitance of the membrane prolongs the effects of a first signal and then allows the second signal to add (Fig. 5). Due to the gradual fall-off, this signal summation will be greatest at the earliest times. In this way, signal summation provides coincidence detection. When two signals arrive at the same time – i.e., when they coincide – the resulting signal will be largest. As the timing of the two signals becomes more separate, the peak of the signal is reduced. Note that the peak of the second signal in Fig. 5 is directly related to the voltage amplitude at the time when the signal begins. This is linear summation. In general, real biological signals are somewhat more complicated, so that summation is nonlinear: the total signal may be either greater or less than the total amplitude predicted by summing the two signals individually.

Transformation #5: From One Membrane Patch to Many – Compartmental Modeling

The patch of membrane we modeled can now be put together with other patches of the membrane to make complicated dendritic trees comparable in appearance to neurons. These dendritic trees are modeled using compartment modeling. Each compartment is an RC circuit similar to Fig. 2. These individual compartments are then connected on the cytoplasmic side (inside) by resistors. As before, the outside is all connected to the ground. Different inputs (synapses) can be located in different compartments, placing them at different locations in the dendritic tree. In general, the further an input is from the soma, the major integrative location of the cell, the less

influence it will have on the output of the cell since the action potential is generated near the soma.

In order to build a model of a real neuron, we would fill a neuron with dye to make the dendritic tree easily visible under the microscope. We would then measure the lengths and diameters of dendrites and map out the branching pattern. A cartoon picture of a typical neuron is shown in Fig. 6a. Using these measurements, we can assign cylindrical compartments. The soma or cell body is in reality a roughly spherical or pyramidal structure. However, it is just going to end up as a bunch of conductances and a capacitance in the circuit model. Therefore, we can represent it as a cylinder or a sphere or anything else as long as we preserve its surface area. (More surface area will translate into more capacitance and more conductance.)

In the context of numerical integration, the spatial division of dendrites into small cylinders of length Δx is analogous to the temporal division of duration into subdivisions of Δt. The quality of any numerical integration depends on making the time steps Δt short enough so that the change in state variables (here the different voltages in the different compartments) during a single time step is insignificant. If the time steps are too long, then the approximation will be inaccurate. We can test for adequate approximation by trying progressively smaller time steps. At the point where the approximation is accurate, reducing the time step further will not alter the

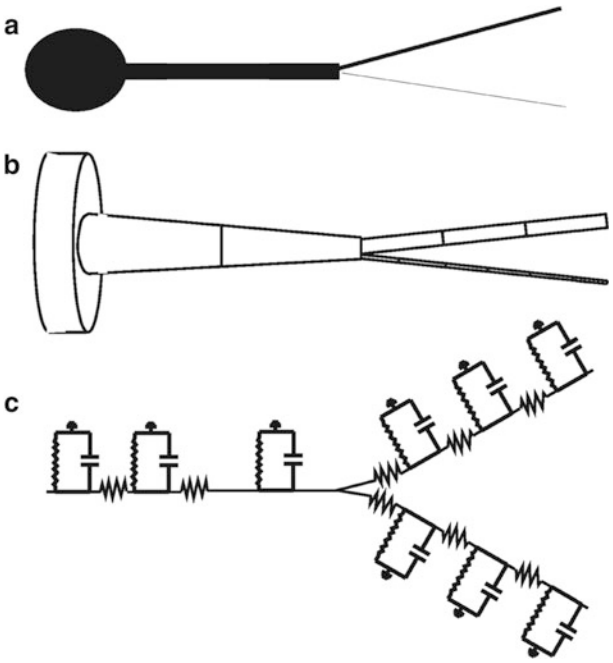

Fig. 6 Three representations of a compartmental model: (**a**) schematic anatomy, (**b**) cylindrical compartmentalization, and (**c**) equivalent circuit model. Each of the individual RC circuits represents a single patch of membrane, which is connected to the next patch by a resistor representing the longitudinal resistance

trajectory substantially. Similarly, the quality of a compartment model depends on making the spatial steps (cylinder lengths, Δx) small enough that the change in voltage over the length of the cylinder is insignificant. This can be tested by choosing smaller cylinders. Note that one wants to use the largest space and time steps that still give accurate results since smaller steps will increase simulation time.

The major difference between the compartmental model and the resistor-capacitor model of Fig. 2 is the longitudinal resistance represented by the resistors between the individual patches of membrane representation. This longitudinal cytoplasmic resistance restricts the flow of current along the dendrite. The narrower the dendrite, the higher its resistance will be. Wide cylinders allow more ions to pass, giving less resistance, less signal drop-off, and faster signal transmission. Because thin cylinders have high resistance, they produce a large voltage drop and must be represented by more compartments than are used with broad cylinders. As before, the voltage drop-off can be calculated using Ohm's law. The algebra for this circuit is similar to what we did in the prior section. But now we have a lot more equations, and we really must use a computer in order to do the calculations.

Transformation #6: From Passive to Active

The compartmental model of the prior section is called a passive membrane model. It reacts passively to signals by charging and discharging, as shown in Fig. 5. It is passive in the sense that the system itself does not add anything to the signal but simply filters it – converting a current or conductance signal into a voltage and prolonging it due to the time constant. Greater complexities arise as we go to an active model. Active means that some of the ion channels, represented by the pores in Fig. 1 and by the resistors in Fig. 2, are now not static but change their resistance due to some influence. This influence is usually either chemical or electrical. However, the influence can also be mechanical, as it is for the pressure sensors used in the skin and in hearing.

Neurons were long known to generate an action potential or spike in the axon. This is an active process: a relatively small signal that produces a much larger spike based on activity in the membrane. In the 1950s, Alan Hodgkin and Andrew Huxley worked out the ionic basis of the action potential and developed a mathematical model for this process. Their work can be regarded in retrospect as the beginning of computational neuroscience. It remains the cornerstone for much neural modeling today. The focus of the original research was on two types of ion channels (the pore in Fig. 1) from a squid axon. Since that time, it has become apparent that there are many different kinds of ion channels that differ in their responsiveness (to chemicals, voltage, pressure) in the ion or ions that they carry (Na^+, K^+, Ca^{2+}, Cl^-) and in the time course and amplitude of the response. Although more precise computer models have been developed to describe the operation of these pores, the Hodgkin-Huxley model is still most commonly used in neuron modeling because the more complex models are too computationally intensive. In the context of multiscale modeling, the Hodgkin-Huxley model represents a simplification of these more complex models.

However, this simplification preceded the development of the sophisticated models rather than being a product of them.

The Hodgkin-Huxley version of the parallel conductance model uses the same passive components (the R and the C) and adds the active components, the rheostats (Fig. 7). We note here a change in the way the passive components are laid out as well. The constant resistor, labeled here *g*, now is in series with a battery, symbolized by the two parallel lines of unequal length (two lines of equal length symbolize a capacitor). Each of the variable resistors (a resistor symbol with a line through it is a variable resistor or rheostat) also has a battery associated with it. All of these batteries are set to different voltages, according to the electrical potential (electrical potential or just potential is synonymous with voltage) produced by energy-dependent pumps that move ions across the membrane. For example, Na^+ is pumped out of the membrane, causing it to have a higher concentration outside than inside. This creates a concentration gradient trying to cause Na^+ to flow back into the cell and an opposing electrical gradient which is therefore positive inside and negative outside.

The equation that describes the relationship of battery strength to concentration difference is called the Nernst equation. The sodium battery in Fig. 7 is therefore shown with the positive pole pointing inward toward the cytoplasm. Notice that the different ions created different batteries, denoted as sodium battery, potassium battery, etc. These batteries function independently and do not interfere with one another. The simple rule for interpreting this circuit is that the more the rheostat is open (conducting, allowing current flow), the more the battery that sits in series with it will affect that overall voltage difference between outside and inside. To see why

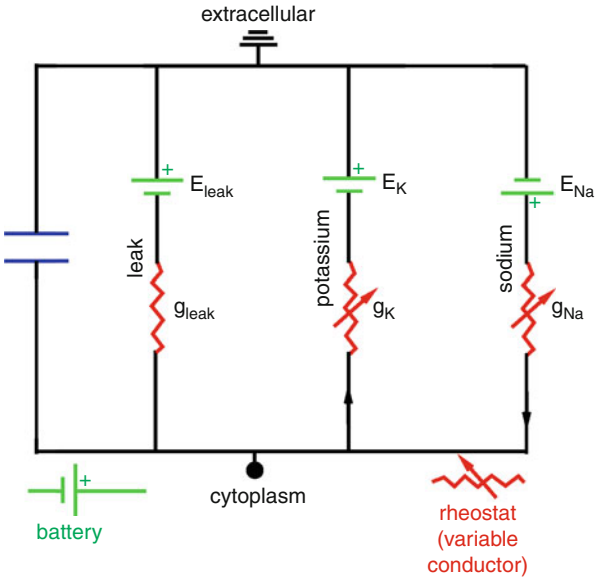

Fig. 7 Parallel conductance model of the membrane. Like Fig. 2 circuit but now with more resistors, including variable resistors (rheostats) as well as fixed ones. All of the resistors are now in series with batteries (*green*)

imagine the rheostat was completely closed. The battery would then be sitting at a "dead end" and thus would not have any impact at all on the rest of the circuit.

At rest, only the leak conductor is open, so the leak battery fully determines the potential, called the resting membrane potential. This is a negative voltage that typically sets the resting membrane potential at about −65 to −70 mV relative to ground. As other rheostats open, their associated batteries begin to influence the membrane potential. This is the source of the various signals that are measured (Fig. 8). Signals that are positive (upgoing) are generally excitatory, while signals that are downgoing are generally inhibitory. Positive signals are called depolarizing, and negative are called hyperpolarizing. Hyperpolarization and depolarization are not symmetrical. The strongest negative batteries can only pull the potential down by about −20 mV, but the strongest positive batteries can pull up to about 100 mV above rest. Artificially, one can move the membrane beyond these bounds by injecting or withdrawing current.

The key to the model mechanism lies in the rheostats. These will increase or decrease their conductance in response to voltage change, leading to positive or negative feedback loops. In the resting condition of the model, the sodium and potassium rheostats are turned off. Since these two lines are not conducting, the associated Na^+ and K^+ batteries have no effect on membrane voltage. The calculations for the parallel conductance model are similar to those for the RC model, except that we have to consider the batteries. As in the RC model, Ohm's law gives a resistive current equal to conductance times membrane voltage. As before, this can be written as $I_R = gV_{memb}$. The amount of current flowing through a given rheostat will depend on (1) the conductance of that rheostat and (2) the difference between the potential of its associated battery and current membrane potential. For the leak

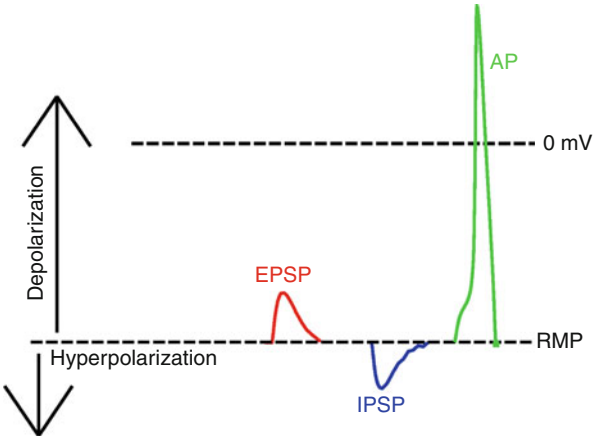

Fig. 8 Resting membrane potential (RMP) is typically about −65 mV (inside negative). The membrane can be depolarized as much as 120 mV or hyperpolarized as much as −30 mV from rest. Excitatory postsynaptic potentials (EPSPs, *red*) depolarize; inhibitory postsynaptic potentials (IPSPs, *blue*) hyperpolarize. Action potentials (APs, *green*) are large, brief (1–2 ms long) depolarizations that can overshoot 0 mV, temporarily reversing membrane polarity

conductance, $I_{\text{leak}} = g_{\text{leak}}(V_{\text{memb}} - E_{\text{leak}})$, where E_{leak} is the potential of the leak current battery, usually about −75 mV. Similarly, $I_{\text{Na}} = g_{\text{Na}}(V_{\text{memb}} - E_{\text{Na}})$ and $I_{\text{K}} = g_{\text{K}}(V_{\text{memb}} - E_{\text{K}})$.

All of the currents add up to zero: $0 = I_{\text{C}} + I_{\text{Na}} + I_{\text{K}} + I_{\text{leak}}$. (We are omitting injected current here.) I_{C} is the current due to the membrane capacitor, and each of the others is a current through pores. Therefore, $-I_{\text{C}} = I_{\text{Na}} + I_{\text{K}} + I_{\text{leak}}$. Substituting for the currents gives the parallel conductance equation:

$$\begin{aligned} -C\frac{\Delta v}{\Delta t} &= g_{\text{leak}}(V_{\text{memb}} - E_{\text{leak}}) \\ &\quad + g_{\text{Na}}(V_{\text{memb}} - E_{\text{Na}}) \\ &\quad + g_{\text{K}}(V_{\text{memb}} - E_{\text{K}}) \end{aligned}$$

At steady state, there will be no capacitative current since voltage is not changing:

$$\begin{aligned} 0 &= I_{\text{Na}} + I_{\text{K}} + I_{\text{leak}} \\ &= g_{\text{leak}}(V_{\text{memb}} - E_{\text{leak}}) + g_{\text{Na}}(V_{\text{memb}} - E_{\text{Na}}) + g_{\text{K}}(V_{\text{memb}} - E_{\text{K}}). \end{aligned}$$

Solving this equation for V_{memb} gives the RMP:

$$\text{RMP} = \frac{g_{\text{leak}}E_{\text{leak}} + g_{\text{Na}}E_{\text{Na}} + g_{\text{K}}E_{\text{K}}}{g_{\text{leak}} + g_{\text{Na}} + g_{\text{K}}}$$

This is a version of the Goldman-Hodgkin-Katz (GHK) equation that states that steady state membrane voltage will be the weighted sum of the batteries, with the weighting provided by the conductance associated with that battery. Since g_{leak} is the dominant conductance at rest, it will have the greatest effect on determining the RMP. If a conductance is turned off completely (e.g., $g_{\text{Na}} = 0$), the corresponding battery has no influence. If, on the other hand, a conductance is very high, then the corresponding battery will dominate, e.g., if $g_{\text{Na}} \gg g_{\text{K}}$ and $g_{\text{Na}} \gg g_{\text{leak}}$, then $V_{\text{memb}} \approx \frac{g_{\text{Na}} \cdot E_{\text{Na}}}{g_{\text{Na}}}$; hence, $V_{\text{memb}} \approx E_{\text{Na}}$. This is what happens at the peak of the action potential: the sodium conductance is high so that the membrane potential starts to approach the sodium reversal potential.

As before, we can look at the Hodgkin-Huxley model from the perspective of active biological proteins, as an electronics circuit, as a set of equations, or as a simulation (Carnevale and Hines 2006, Hines et al. 2020). But we can also describe the interaction of the channels in terms of positive and negative feedback systems. We will use this explanation here since it is the most straightforward and does not rely on knowledge of electronics or differential equations. Feedback refers to the detecting of a change that has been brought about by the actions of a system. First, the system acts on the environment. Second, the system detects a change in the environment. This change is the feedback that the system is receiving based on its actions, just as verbal feedback from your instructor will accompany your learning to play tennis. Negative feedback is a property in a system that resists changes. When a change is detected in the environment, the system reduces or reverses its influence on

the environment. The classic example is a thermostat: when it gets hotter, the thermostat stops heating or starts cooling; when it gets colder, it does the opposite. Negative feedback is seen in homeostatic systems. The term "stasis" in homeostasis and "stat" in thermostat both imply a static environment – keeping things at or near a set point. By contrast, positive feedback keeps moving the environment away from a set point. Purely positive feedback systems tend to be bad: think nuclear meltdown. Positive feedback systems are not self-limiting; they are limited by something outside of the system (i.e., dispersal due to an explosion). It can be very useful for a system to mix positive and negative feedback since this way, and it can be very sensitive to small changes in the environment (positive feedback) while still being able to handle large ones (negative feedback).

The Hodgkin-Huxley sodium and potassium channels are voltage-sensitive conductances. They go on and off with voltage change. If positive voltage change creates a current that leads to a more positive voltage change, this would be positive feedback. This is a property of the Na^+ channel. If positive voltage change creates a current that reduces or reverses positive voltage change, this would be negative feedback. This is a property of the K^+ channel. The ion channels are conceptualized as working through switches. Thinking back to the thermostat, we see that it is a system that controls temperature by switching on and off heating and cooling systems. Similarly, the ion channels control voltage by switching currents on and off. For the individual ion channel, the switch is either on or off. However, the rheostat in Fig. 7 represents a large population of individual ion channels. When all of those channels are open, the switch is completely on, represented mathematically by the number 1 in the Hodgkin-Huxley equations. When all of the channels are closed, the switch is completely off, represented by 0. Most of the time, some are on, and some are off, so the system is partway on, represented by some decimal value between 0 and 1.

The Hodgkin-Huxley model is still more complicated since one of the active channels, the Na^+ channel, is controlled by two switches rather than by one. In addition to a regular on/off switch (the "m" switch), it also has a separate dedicated inactivation switch (the "h" switch) that can be viewed as an override system that kicks in when positive feedback goes too far. This leads to a surprising amount of additional complexity since one has to think not only how the "m" switch gets turned on and then off but also how the "h" switch gets turned to off (the override) and then back to the on position. The K^+ channel has only the single on/off switch: the "n" switch.

Turning on the "m" switch activates the Na^+ channel and pushes voltage (V) up to less negative (depolarized) values. Turning on the "n" switch activates the K^+ channel and pushes down (hyperpolarizes). The switches are controlled by voltage. The system produces an action potential (also called a "spike" because of its appearance) because the positive and negative feedback loops are activated in a sequence. The sequencing is produced by the fact that the switches are associated with different time constants and voltage sensitivities: out of T_m, T_h, and T_n, T_m is the smallest, so "m" switches on first in response to depolarization. This causes Na^+ channels to open (i.e., the rheostat begins to conduct), which in turn produces a sharp

upswing in *V* as the circuit seeks to come up to the voltage defined by the Na^+ battery, usually about +45 mV. This depolarization leads to further opening of the channels – the positive feedback response – until the membrane potential reaches +30 to +40 mV. The depolarization now causes the slower "h" and "n" switches to kick in. The "h" switch starts to turn off the Na^+ channels, even as "m" is still turning them on – but since Na^+ is only on if both "h" and "m" are on, the net effect is to turn Na^+ off. The "n" switch starts to turn on K^+ channels, pulling the membrane down toward the value of the K^+ battery, usually around −90 mV. The result of all of this "on"ing and "off"ing is shown in Fig. 9.

The positive feedback during the upswing of the action potential allows the *V* to rise about 100 mV over about 1 ms in a mammal. The rates of all the switches, like all proteins, are temperature dependent. Compared to normal functioning at body temperature, the action potential will be slower and broader in a neuron placed in a dish at room temperature and slower still in a squid neuron kept at the deep-sea temperature of about 6 °C.

Figure 9 is just the tip of a dynamical iceberg. In Fig. 4, we had only one state variable, *V*. In Fig. 9, and we are still only showing one state variable, which obscures the fact that there are four: m, h, n, and *V*. We could show the other state variables on three additional graphs. However, it is often more revealing to graph one state variable against another on a *phase plane* where the trajectories determined by the dynamics will be revealed as loops. But even this representation only reveals two dimensions of this four-dimensional system. In general, as we go to higher dimensions, the difficulty of adequate visualization increases.

In large network models, we can have millions of state variables. These state variables interact in complex ways, making the analysis of these systems complex (Rieke et al. 1999), though not nearly as complex as the analysis of the experimental systems upon which they are based. These are systems of interlocking, linked differential equations. Positive and negative feedback systems coexist with different strengths and different delays in large and small loops. In these entangled systems, it

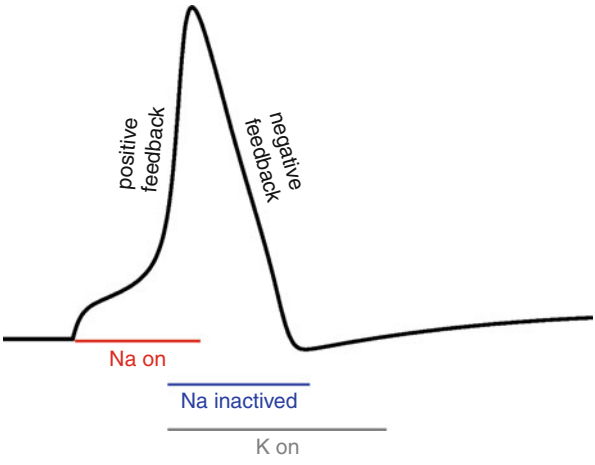

Fig. 9 Positive feedback (*upswing*) followed by negative feedback (*downswing*) shapes the action potential. The time constant of Na^+ inactivation by the "h" switch is approximately the same as that of K^+ activation, so the *downswing* is due to both increased K^+ conductance and reduced Na^+ conductance

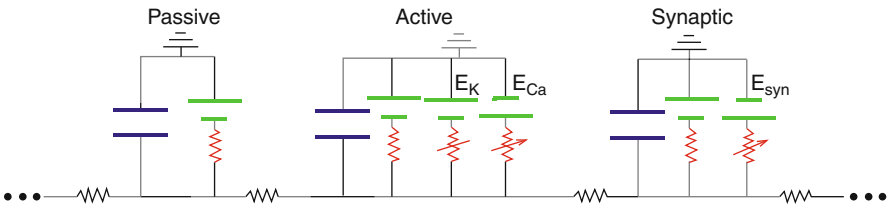

Fig. 10 Three example compartments from a dendrite model. On the circuit diagram, different rheostat branches are distinguished only by the directions of their batteries

is typically not possible to assign clear causality as these cycles and cycles-within-cycles provide many paths of influence. Chasing these state variable interactions around multiple feedback cycles produces proverbial chicken-and-egg predicaments.

When putting together a compartmental model of a particular neuron, neurophysiological data would likely suggest the inclusion of additional voltage-sensitive conductances (rheostats) in some compartments. We will also need to include other rheostats to represent synapses. Figure 10 shows three compartments from a neuron model: one passive, one active, and one synaptic. The active compartment is labeled here as using a Ca^{2+} battery, so this would be set with different parameters than are used with the Na^{+} battery from the Hodgkin-Huxley equation. The synaptic compartment is shown with a depolarizing battery. Therefore, this would be an excitatory synapse. Biologically, the associated rheostat would be triggered by a chemical. However, we are not modeling chemicals, so in our context, the trigger would just be a signal. In a network model, this signal might be received from another neuron when that neuron spikes.

Putting It All Together

Now we have all the tools to model a neuron. If we start with a passive neuron model and provide synaptic inputs, we can demonstrate that inputs far from the soma will have less effect on the soma than will those nearby. In Fig. 11, we stimulate the neuron by initiating excitatory postsynaptic potentials (EPSPs) at different locations to see how the signal spreads. Looking at the soma trace (second from bottom), we see that EPSPs triggered at different locations have different effects at the soma. The effect at the soma is important since this is near the primary integrating area where the output spike will be generated (the axon initial segment). The first EPSP is at the bottom, as indicated by the arrow on the corresponding trace. This EPSP is still seen at the soma but appears smaller and somewhat delayed. Similarly, the second EPSP, generated at the soma, is seen as smaller and delayed at other locations in the cell. The degree of spread is determined by the passive membrane parameters. The increased capacitance will favor the spread of longer signals compared to short ones. Membrane leakiness (membrane conductance) will reduce spread since signals leak out into the extracellular space. Longitudinal (cytoplasmic) resistance will also reduce spread.

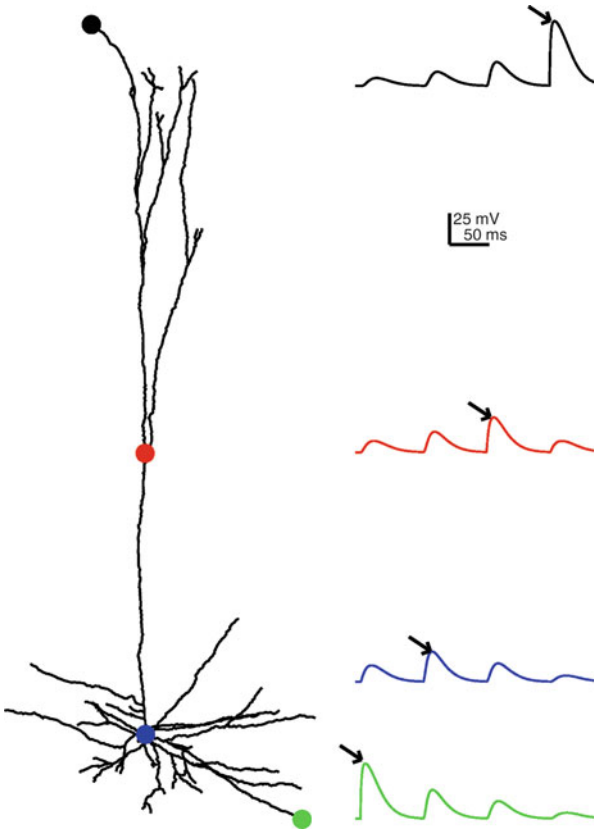

Fig. 11 Signal spread in a multicompartment neuron model. Each of the colored dots represents a location of both stimulation and recording. One stimulus was applied to each location, moving from *bottom* to *top*. The color of each voltage trace corresponds to the identically colored location on the neuron. *Arrows* on the voltage trace indicate which stimulus was applied at that recording location; the other three are the result of propagation. In general, the further a signal travels from the site of stimulation, the smaller its amplitude will be

Notice that the EPSPs initiated at the ends are larger than those triggered at other locations despite the fact that the same synaptic conductance was used at each location. The difference in response is due to the fact that current has only one direction to travel in at an end. It, therefore, tends to "pile up" instead of leaking away in two directions down the dendrite. In electrical terms, these terminal locations have relatively high input impedance. Impedance refers to any obstacle to current flow. In a dendrite, resistance provides a constant impedance, while capacitance provides a frequency-dependent impedance. A capacitor has an impedance inversely proportional to frequency: high for low-frequency signals and low for high frequency. This produces the opposite effect on signal passage down the dendrite since high-frequency signals are shunted across the membrane to ground, while low-frequency signals are allowed to pass through only slightly attenuated (Fig. 12). Sinusoidal signals like those shown here are sometimes applied to cells in order to test their responsiveness. Biological signals, EPSPs, approximate a half cycle (one up and one down) of such a signal. The same effect would be seen with these signals: a long-duration EPSP will travel farther than a short-duration EPSP.

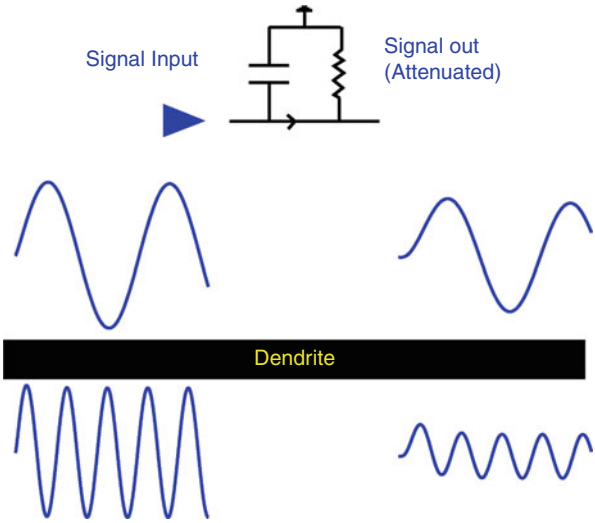

Fig. 12 Signal frequency determines signal passage (*left* to *right)* down a dendrite. High-frequency signals (*top*) are more attenuated: lower amplitude for the high-frequency signal on *right*

In addition to increasing the size of an EPSP at a distal dendrite, high terminal input impedance also reduces the drop-off of the EPSP going away from the soma, compared to the drop-off of an EPSP going toward the soma. These two effects, the increased size of a distal EPSP and the increased drop-off toward the soma, tend to cancel out. Therefore, a distal input arriving at the soma is about the same size as a somatic input arriving at a distal dendrite. High distal input impedance produces a large distal EPSP (top trace, fourth EPSP). This large EPSP is substantially decremented when seen at the soma (third trace, fourth EPSP). Going in the other direction, the somatic EPSP is relatively small due to lower input impedance (third trace, second EPSP), but signal fall-off from the soma to the distal dendrite is relatively small (top trace, second EPSP). In this way, differences in input impedance are partially balanced by the asymmetry in the transfer of signals in these passive models.

If we now make the soma into an active compartment with Hodgkin-Huxley channels, we can trigger the distal dendrite and see a spike in the soma. In Fig. 13, an EPSP is triggered in the distal dendrite that then travels down the dendritic tree. Only the soma compartment is active; all dendrite compartments are passive. Note that the progress of the signal down the dendritic tree (downward arrow) is not entirely smooth and is not quite the same as the backward propagation of the action potential back up (upward arrow). Delays in signal propagation tend to occur where there is branching.

Biologically, dendrites are not passive but instead include many voltage-sensitive channels. Unfortunately, it is not clear exactly which channels are present in particular cell dendrites and whether these channels will tend to have an overall augmenting effect (as would be the case with Na^+ and Ca^{2+} channels) or an overall attenuating effect (with K^+ channels) on signal passage. Furthermore, these dendritic voltage-sensitive channels can be modulated by phosphorylations and by the

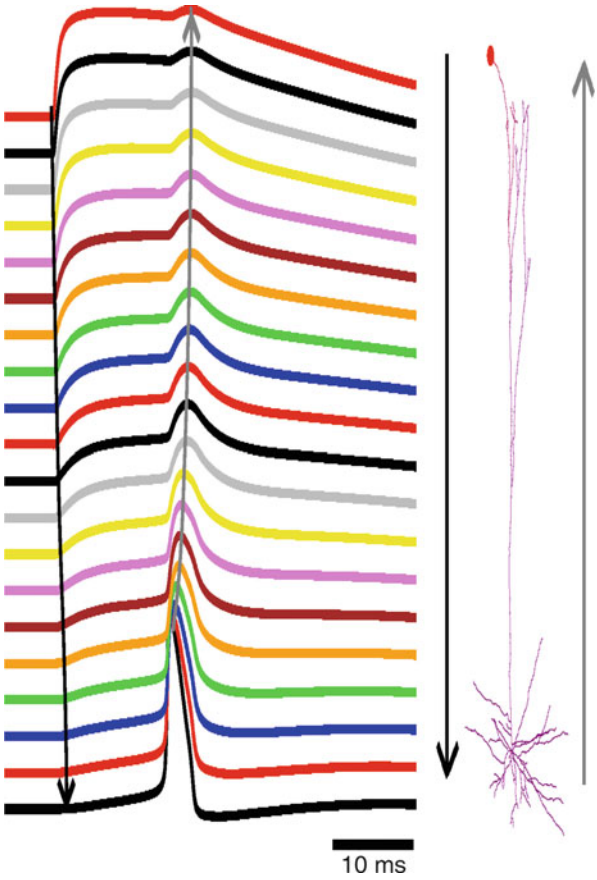

Fig. 13 Strong distal activation (*red dot* on neuron) generates a signal that propagates passively down to the soma (*black downward arrows*), where an action potential is generated, which then propagates passively back up the dendritic tree (*gray upward arrows*). Each voltage trace (*left*) was recorded at the corresponding vertical position in the dendritic tree. Notice that neither of the signals propagate at a constant velocity – i.e., the *black* and *gray lines* are not completely straight

presence of other chemical signals, allowing them to play different roles under different circumstances potentially. In Fig. 14, we give an example where the dendrites are signal-augmenting through a combination of Na^+ and K^+ channels. We provided the same stimulus as in Fig. 13. The dendrites, in this case, have the same Hodgkin-Huxley channels that are present in the soma but with the Na^+ channel at about one-eighth density. The most distal compartments, where the signal is given, are left passive. The voltage profile is now more complicated, with evidence of some partial backpropagation of signal from a point partway down the dendrite. This complexity with just a single input signal begins to suggest the complexities of signal integration that could occur with the multiple inputs that real pyramidal cells are being continuously exposed to.

There are other approaches to describing the Hodgkin-Huxley model, in addition to five or six used in this chapter. For example, one can use complex graphical representations that allow us to look at several dimensions of the dynamics at once, phase plane representations. One can then apply mathematical techniques to help us

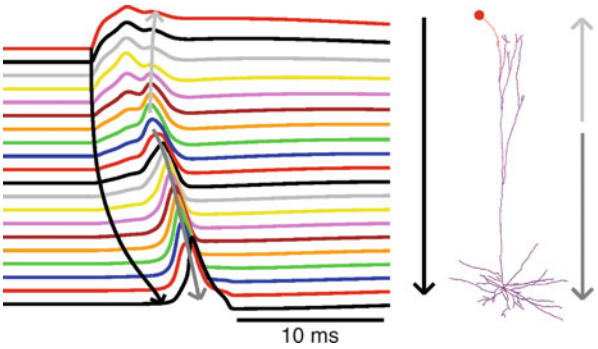

Fig. 14 Activation as in Fig. 13, except with active dendrites, showing much more complicated wave propagation. Along with an initial activation traveling down to the soma (approximately traced by *black downward arrow*), an active depolarization begins partway down the dendritic tree and propagates in both directions – to the soma (*dark gray downward arrow*) and back up through the dendritic tree (*light gray upward arrow*)

understand the trajectories on the phase planes: descriptions of nullclines and of the space of solutions as a field (Koch 2004).

Chemophysiology

Computational neuroscience has traditionally focused on electrophysiological phenomena, action potentials and firing rates, whereas systems biology has had a focus on the chemical properties, taking a system dynamics perspective of cells and chemical signaling networks. Recent developments are beginning to bridge the gap between the two perspectives. As more experimental methods to measure the concentrations of neuroactive substances – such as enzymatic biosensors, calcium-sensitive dyes, chloride imaging, and fast-scan cyclic voltammetry – have become available, there is more data to connect chemophysiology with electrophysiology. An additional technical advance has been the great increase in computational power of High Performance Computers (HPCs), and widespread HPC availability via resources such as Google Cloud and the freely-available Neuroscience Gateway. These allow for more complex simulations combining intracellular chemophysiology (the complex intracellular mechanisms of second messenger signaling and cascades) and extracellular chemophysiology (neurotransmitter and toxin spread) with electrophysiology in a network context. New scientific software, libraries and simulation platforms have been developed to facilitate the development of such simulations, including STEPS, the NEURON simulation platforms' reaction-diffusion (rxd) module, NeuroRD, MOOSE and NetPyNE.

Calcium is an important second messenger for many cell types and plays a multitude of roles. As it is such a potent signal, calcium in neurons is heavily regulated by buffering and uptake to intracellular organelles, the endoplasmic reticulum (ER) and mitochondria. This allows cells to maintain very low free

calcium concentrations in the cytosol of ~60 nM, compared to ~1 mM in the extracellular space. Tight regulation of intracellular calcium greatly limits diffusion of calcium in dendrites, so that other mechanisms are responsible for calcium signal spread in the spatially extended dendritic arbor – calcium-induced calcium release (CICR). CICR utilizes stored calcium in the ER to produce a calcium wave that can spread hundreds of microns through the dendrite. The mechanism for concentrating calcium in ER is the sarco/endoplasmic reticulum Ca^{2+}-ATPase (SERCA) pump. A major mechanism for calcium-induced release is calcium involvement in the activation of inositol trisphosphate (IP_3) receptors (IP_3R). IP_3 is one of the second messengers that neurons produce in response to glutamatergic excitatory activation.

The schematic (Fig. 15a) shows a model for the apical dendrite with the voltage-dependent sodium, potassium, and leak channels as discussed in the previous sections. In addition, the AMPA receptor (AMPAR), one of the two main types of excitatory glutamate synaptic receptors, provides activation so that calcium enters the cell via the three types of voltage-gated calcium channels (VGCC) modeled here. Each type has distinct dynamics: T-type – low voltage activation; N-type – high voltage activation and inactivation; and L-type high voltage, long-lasting activation. The model was equipped with the SERCA and IP3R necessary to produce CICR.

Two examples are shown (Fig. 15b), one with AMPAR stimulation (primed, 150 pulses with 25 ms interspike interval) and one without (not primed). In each case

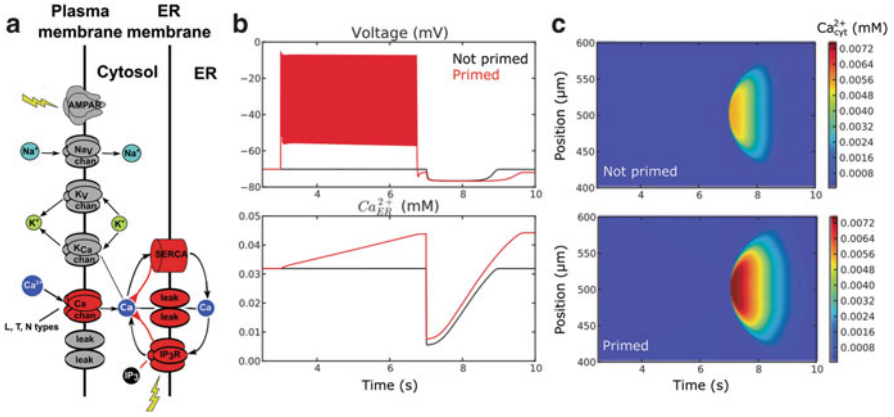

Fig. 15 Computational model of calcium-induced calcium release in a section of the apical dendrite. (**a**) Schematic of the model mechanism, the lightning bolts indicate external stimulation. The model includes; sodium and potassium channels, voltage-dependent calcium channels, passive leak, and AMPA receptor as well as calcium-dependent potassium channels, which hyperpolarize the cell after calcium influx. (**b**) The membrane potential in the primed (150 pulses with 25 ms interspike interval) and not primed stimulation (top). ER calcium concentration (bottom) in the two cases shows calcium is loaded into the ER by repeated depolarizations. At 7 s the IP_3R is stimulated by adding 2.5 mM of IP3, leading to a rapid release of calcium via the IP_3R. Calcium release results in hyperpolarization (top), but the primed case lasts ~2 s longer. (**c**) The two calcium waves in the dendrite. The primed calcium wave is of larger amplitude and duration and travels ~70 μm further. (Figure adapted from Neymotin et al. 2015)

at 7 s there is a 2.5 mM IP_3 stimulus that causes the IP_3R to release calcium from the ER, causing a localized wave of calcium to spread through the dendrite. This in turn opens K^+ channels and produces hyperpolarization of the membrane. In the unprimed case, the calcium wave spreads ~150 μm, whereas in the primed case, the wave spread ~220 μm and the hyperpolarization lasted around 2 s longer. The reason for this is the AMPAR stimulation allowed extracellular calcium to enter the cytoplasm, which was then moved by the SERCA to the ER, increasing calcium concentration in the dendrite from 30 μm to 45 μm, creating a larger wave when the calcium was released by the IP3R. This model shows how the dynamics of chemical signals in the neuron alter the electrophysiological response of the cell.

This model has been developed to explore the effect of calcium stores on persistent network activity. Persistent neuronal activity (lasting several seconds) may underlie functions such as short-term working memory and motor preparatory sets. The idea is that the network will encode an input pattern. A measure of how effectively it has encoded the pattern is the *firing rate discrimination* (FRD), the ratio of the firing rate of neurons in the pattern to those not in the pattern.

Here we describe how a network can support input pattern representations using interacting chemical and electrical signaling. The model of 776 neurons (Fig. 16) produced persistent network activity driven by a somewhat paradoxical combination of recurrent excitation and recurrent inhibition (to trigger hyperpolarization-activated cyclic nucleotide-gated channels: HCN). A metabolic glutamatergic receptor (mGluR) produced IP_3 in response to synaptic stimulation, which not only supported CICR but also shifted the activation of the HCN channel, which helped

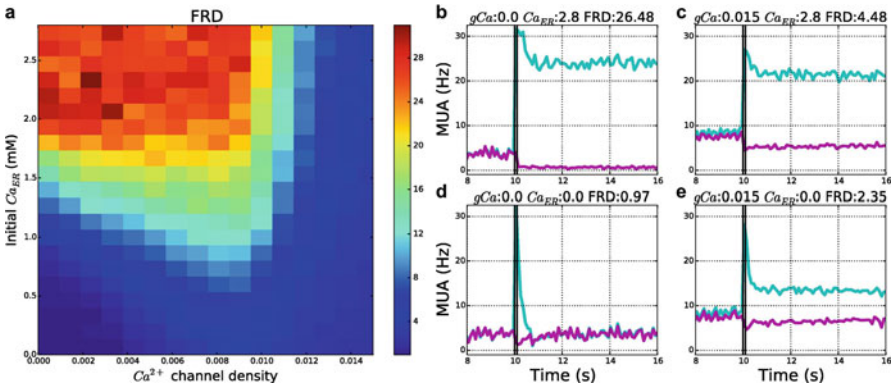

Fig. 16 Firing rate distinction depends on both external (VGCC) and internal (ER) calcium stores, determined respectively by VGCCs density and ER. (**a**) 21 s simulations were run varying the density of VGCCs (x-axis) from 0 to 0.015 nS/cm^2 (levels). The four multiunit activity (MTU) examples are taken from four corners of (**a**). (**b**) High internal Ca^{2+} stores in the absence of VGCCs allows for high FRD (26.48), upper left of (**a**). (**c**) High internal Ca^{2+} stores and high density of VGCCs produces moderate FRD (4.48), upper right of (**a**). (**d**) No internal Ca^{2+} stores in the absence of VGCCs produce low FRD (0.97), lower left of (**a**). (**e**) No internal Ca^{2+} stores and high density of VGCCs produces moderate FRD (2.35), lower right of (**a**). (Figure reproduced from Neymotin et al. 2016)

provide the support for continued network activity. This model showed the influence of VGCC density (from 0 to 0.015 nS/cm^2) and initial calcium stores (0–2.8 mM) on the ability of the network to encode the pattern (Fig. 16a). FRD increases with available calcium stores (Fig. 16a y-axis) as these only contribute to post-stimulus firing. FRD has an inverted-U relationship with VGCC density (Fig. 16a x-axis), at low to moderate levels, an increase in calcium influx will increase post-stimulus firing, but at higher levels, the calcium will also increase firing in both stimulated and unstimulated populations, leading to poorer FRD. Without ER Ca^{2+} or VGCCs there is insufficient increase in cytosolic Ca^{2+} to induce a post-stimulus response (Fig. 16d), greater VGCC density increases both populations firing rates leading to weak suppression of the unstimulated population (Fig. 16e). With high VGCC density and high ER stores lead to a substantial increase in FRD, as post-stimulus firing rates increase, leading to greater suppression of the unstimulated population. The largest FRD comes from low to moderate VGCC density and high ER stores (Fig. 16b). This model suggests the importance of intracellular calcium dynamics contributed to persistent network activity.

Extracellular Space and Spreading Depression

Although ions are exchanged with the extracellular space (ECS) in the prior models, the extracellular concentrations are held constant. However, the ECS of neural tissue is an active medium, with a multitude of physiological, pharmacological and pathological agents, including neuromodulators, ions, inflammatory cells, oxygen, *etc.* These agents will influence both the electrophysiology and chemophysiology of the cells. Modeling the ECS depends in part on the scale of interest. At the microscale, fine meshes can be constructed from electron microscopy reconstructions, and the diffusion of single particles can be simulated (for example, using the MCell simulator). At the mesoscopic scale (more appropriate for models of networks) a volume-averaged approach is adopted, where the tissue is described by its diffusion characteristics, the tortuosity (the average ratio of the increase in path length due to obstacles) and volume fraction (the proportion of free space in which substance can diffuse). These mesoscopic scale diffusion characteristics have been measured for different species and brain regions in physiological and pathological conditions (Syková and Nicholson 2008).

Spreading depolarization (SD) is a wave of depolarization of neurons that propagates in the gray matter of the brain at a speed of ~2–7 mm/min for a duration of around 1 min. SD is associated with several pathological conditions, including migraines, traumatic brain injury, epilepsy and ischemic stroke. It can be triggered in experiments with a localized increase in extracellular potassium. Simulations have been used to understand the large change in ion gradients during SD (Somjen 2004). An early mechanistic model attributed the depolarization to extracellular K^+ (Grafstein's hypothesis). Here this mechanism is simulated, 90,000 neurons with Hodgkin-Huxley like dynamics placed in 1 mm^3 of ECS, with the initial extracellular K^+ concentration raised to 40 mM in a sphere of 100 μm at the center. The model produced a wave of extracellular K^+ (Fig. 17a) and neuronal depolarization

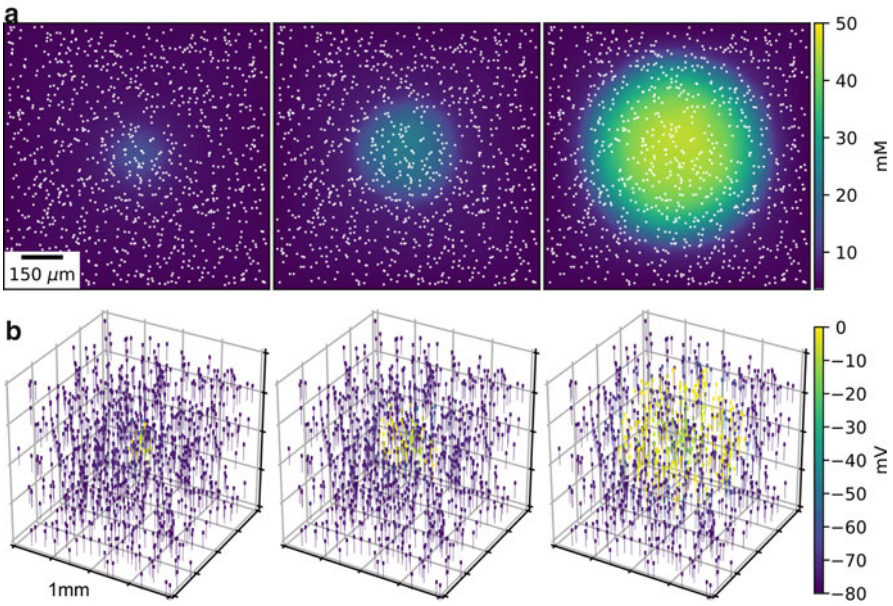

Fig. 17 SD wave with time points at 10, 20, 30 s and concentrations averaged over the depth of 1 mm^3 of ECS. (**a**) Extracellular K^+ with glial uptake (modeled as a reaction) and a fixed concentration at the boundary. The white dots show the location of 1000 (of 90,000) neurons. (**b**) Membrane potential, for example, neurons. (Figure adapted from Newton et al. 2018)

(Fig. 17b) characteristic of SD. The high extracellular K^+ concentration depolarized neurons providing additional K^+ to feed the SD wave – a positive feedback loop.

Outlook

We have covered some of the basic techniques that allow us to generate computer models of single neurons. These many techniques – biophysics, biochemistry, electronics, differential equations, algebra, numerics, and systems engineering – provide a rounded view of single neuron dynamics. Looking at the same phenomenon from so many different perspectives provides an understanding that cannot be gained by looking at only one. Similarly, experimenting with the simulation by testing parameter variations and observing the effects, as we did in comparing Figs. 13 and 14, gives further insight. One begins to develop an intuition as to what the biological systems are capable of and how they sometimes react in unexpected or paradoxical ways. The addition of chemophysiology to electrophysiology provides another layer of complexity and another set of numerical calculations, which helps us connect system biology's metabolism and signaling pathways to the more familiar classical electrophysiology.

The payoff for all of this hard work can be appreciated by considering the well-known parable of the blind men who meet an elephant – one feels the trunk, one a leg, another a tusk, etc. – and they give widely discrepant descriptions of the beast. None of them knows anything useful about elephants, but if they pool their knowledge, they may be able to create a passable picture. Similarly, coming at a model from many angles permits us to come closer and closer to understanding the thing itself. We have neither the concepts nor the mental capacity to wrap our brains around all of this complexity and see nature as it really is. Instead, we use these different models as tools to pick up different clues to this underlying reality. As we move back and forth between representations, we gain deeper insights.

Glossary

Compartmental model A model with connected isopotential compartments representing a dendritic tree or other neural structure.

Dynamical system A system of interrelated values that change in time.

Parallel conductance model Model of neural membrane featuring rheostats, resistors, and a capacitor in parallel.

State variable The variables that change with time in a dynamical system.

References

Arbib MA (1998) The handbook of brain theory and neural networks. MIT Press, Cambridge, MA

Carnevale NT, Hines ML (2006) The NEURON book. Cambridge University Press, Oxford

Churchland PS, Sejnowski TJ (1994) The computational brain. MIT Press, Cambridge, MA

Dayan P, Abbott LF (2001) Theoretical neuroscience. MIT Press, Cambridge, MA

Koch C (2004) Biophysics of computation: information processing in single neurons. Oxford University Press, Oxford

Hertz JA (2018) Introduction to the theory of neural computation. CRC Press

Hines M, Carnevale T, McDougal RA (2020) NEURON simulation environment. In: Dieter J, Ranu J (eds) Encyclopedia of computational neuroscience. Springer, New York, NY, pp 1–7. https://doi.org/10.1007/239978-1-4614-7320-6_795-2

Lytton WW (2002) From computer to brain. Springer, New York

Neymotin SA, McDougal RA, Sherif MA, Fall CP, Hines ML, Lytton WW (2015) Neuronal calcium wave propagation varies with changes in endoplasmic reticulum parameters: a computer model. Neural Comput 27(4):898–924

Neymotin SA, McDougal RA, Bulanova AS, Zeki M, Lakatos P, Terman D, Hines ML, Lytton WW (2016) Calcium regulation of HCN channels supports persistent activity in a multiscale model of neocortex. Neuroscience 316:344–366

Newton AJH, McDougal RA, Hines ML, Lytton WW (2018) Using NEURON for Reaction-Diffusion modeling of extracellular dynamics. Front Neuroinf 12:41

Syková E, Nicholson C (2008) Diffusion in brain extracellular space. Physiol Rev

Rieke F, Warland D, de Ruyter R, Steveninck V (1999) Spikes. MIT Press, Cambridge, MA

Somjen GG (2004) Ions in the brain: normal function, seizures, and stroke. Oxford University Press, Oxford

Trappenberg T (2010) Fundamentals of computational neuroscience. Oxford University Press, Oxford